

**SURFACE LEVEL
SOLAR ULTRAVIOLET-B RADIATION
AT PENANG**

by

ARUNASALA PANDY A/L KARUPPUSAMY

June 2006

Thesis submitted in fulfilment of the requirements
for the degree of **Doctor of Philosophy**

ACKNOWLEDGEMENTS

I wish to express my thanks to my Main Supervisor Associate Professor Dr. Fauziah Sulaiman for her help and guidance throughout the course of my study. Her essential and constructive comments have enabled me to successfully complete this research thesis. Thanks also to my ex-supervisors Professor Dr. Mohammad Ilyas and Professor Dr. Syed Idris Bin Syed Hassan.

My thanks also go to the present and past Deans of the School of Graduate Studies and School of Physics for their patience, help and advice during those stressful and trying moments mid-way through my research study. I would like to gratefully acknowledge the help and support of all the Staff at the Astronomy and Atmospheric Science Research Unit, USM. Thanks also to Associate Professor Dr. Mohd Nawawi Mohd Nordin for helping me to obtain meteorological data from MMS. I am also grateful to the Ministry of Education, Malaysia for granting permission to pursue this post-graduate programme.

For access to the TOMS total column ozone data, I wish to thank Dr. Jay Herman and the Laboratory for Atmospheres, NASA/Goddard Space Flight Center. Thanks also to Dr. Anatoly Tsvetkov, WRDC Laboratory Chief and Steve Wilcox at the World Radiation Data Center for providing solar radiation data for some major cities in Malaysia and around the world. I am also grateful to Dr. Sasha Madronich of the National Center for Atmospheric Research at Boulder, Colorado (USA). I would also like to thank the Malaysian Meteorological Services (MMS) for providing a variety of meteorological data. I wish to acknowledge the help rendered by Professor Azni Zain Ahmed from Universiti Teknologi MARA, especially in giving me an insight on solar radiation research in Malaysia.

The experimental part of this research has been supported through an IRPA funded ozone and UV project to Professor Dr. Mohammad Ilyas by the Ministry of Science, Technology and Environment, Malaysia.

Lastly, my special thanks to my wife Sylvia and my children Vennila Aurora and Aeron Marvel for their patience, love, encouragement and emotional support throughout my study period. I regret only that my parents, who gave me self-belief and confidence are not around. I dedicate this work to them.

TABLE OF CONTENTS

	Page
Acknowledgements	ii
List of Tables	vii
List of Figures	viii
Nomenclature	xi
Terminology	xiii
Abstrak	xiv
Abstract	xvi
Chapter 1 Introduction	1
1.1 Attenuation of Surface Level Solar Ultraviolet Radiation	4
1.2 Relevance of Solar Ultraviolet Radiation Measurements	6
1.3 UV Measurements	8
1.4 Research Objectives	10
1.5 Thesis Overview	11
Chapter 2 Experimental	12
2.1 Introduction	12
2.2 Types of Radiation Instruments Used	15

2.2.1	Solar UV-B Radiation	15
2.2.2	Solar UV-A Radiation	21
2.2.3	Global Solar Radiation	24
2.2.4	Diffuse Solar Radiation	27
2.3	Instrument Activation	27
2.4	Instrument Maintenance and Data Acquisition	31
2.5	Calibration and Stability of the Photometers	34
2.6	Data Selection	41
Chapter 3 UV-A, Global and Diffuse Solar Radiation		46
3.1	Daily Total Global Radiation	48
3.1.1	Time Series of Daily Total Global Radiation	48
3.1.2	Time Series of Monthly Mean Global Radiation	51
3.2	Diurnal Variations	57
3.3	Noon Time Irradiances	62
3.4	Global Radiation for Cloudless Skies	66
3.4.1	Extraterrestrial Daily Total Global Radiation	66
3.4.2	Identification of Cloudless Days	68
3.4.3	Time Series of Global Radiation for Cloudless Skies	69
3.5	Calculations of Cloudless Sky Global Solar Radiation	73
3.6	Diffuse Solar Radiation	75
3.6.1	Daily Total Diffuse Radiation	77
3.6.2	Half-hourly Diffuse Solar Irradiance	77

3.7	Solar UV-A Radiation	80
3.7.1	Daily Total UV-A Radiation	80
Chapter 4	Solar Ultraviolet-B Radiation	87
4.1	Introduction	87
4.2	Results and Discussions	87
4.2.1	Seasonal Variations	87
4.2.2	Diurnal Variations	94
4.2.3	Noon Time UV-B Irradiance	100
4.2.4	UV-B Radiation for Cloudless Skies	106
4.2.5	UV Index	108
4.3	Comparison with Other Sites	109
4.4	Introduction	113
4.4.1	Total Ozone Column	114
4.4.2	Surface Level Ozone	117
4.4.3	Clouds	119
4.4.4	Aerosols	122
4.4.5	Humidity	122
4.4.6	Temperature	123
Chapter 5	A UV-B Model for Cloudless Sky	124
5.1	Introduction	125
5.2	UV-B Spectral Model Description	128
5.2.1	Direct Spectral Irradiance	132

5.2.2	Diffuse Spectral Irradiance	141
5.3	Spectral Model Assessment	146
5.3.1	The Tropospheric Ultraviolet-Visible Model	147
5.3.2	Green's Model	147
5.3.3	Model Comparison	149
5.3.4	Multivariate Analysis	150
Chapter 6	Conclusions	154
References		160
Appendices		
A	Figure 1 Non-linearity (sensitivity variation with irradiance) of CM 11 pyranometer.	175
	Figure 2 The curve of relative sensitivity variation with instrument temperature of a CM 11 pyranometer is in the shaded region. A typical curve is drawn.	
B	Mean half-hourly values of the total solar global irradiance (kW m^{-2}) at Penang in the years 1994-1999.	176
C	Extraterrestrial horizontal daily total global radiation for Penang, H_o (MJ m^{-2}), $S = 1370 \text{ W m}^{-2}$, $D_n = \text{day number}$.	177
D	Mean half-hourly values of the solar ultraviolet-B irradiance (W m^{-2}) at Penang for the years 1994-1995 and 1998-1999.	179
E	Adapted from Madronich	180
F	Surface level erythemal UV-B radiation at Penang in kJ m^{-2} , D_n day number.	181
G	Long term measured monthly mean surface pressure (in mb) at Bayan Lepas (Penang) (1951-1988, 398 months) and Subang (1951-1988, 446 months).	189

LIST OF TABLES

Tables	Page
2.1 Detailed tabulation of conversion factors for total UV-B and erythemal irradiance.	22
2.2 Summary of instruments used in this research.	29
2.3 (a) Calibration of the UVB-1 instrument with a reference unit.	35
(b) Calibration of the TUVR Eppley UV photometer with a reference unit.	42
(c) Calibration of the Kipp & Zonen pyranometer (serial number : 913392) with a reference unit.	43
(d) Calibration of the Kipp & Zonen pyranometer (serial number : 913393) with a reference unit.	44
3.1 Statistical analysis of measured daily total global radiation (in $\times 10^7 \text{ J m}^{-2}$) at Penang according to month and year for the years 1994-1999.	50
3.2 Monthly mean global radiation (in J m^{-2}) at Penang (1994-1999) and some other cities in Malaysia (1989-1993).	50
3.3 Number of identified clear sky days during the period from September 1994 to 4th December 1999.	70
3.4 Percentage of identified cloudless sky days for different years. Selection is based solely on the criteria of $K > 0.6$ and $\alpha_1 < 0.15 $.	70
3.5 Monthly mean daily total UV-A radiation for the period 1994-2001 at Penang. Units are in $(\times 10^5) \text{ J m}^{-2}$.	85
4.1 Statistical analysis of measured daily total UV-B radiation for the 1994-1995 and 1998-1999 period at Penang. Units are in $(\times 10^4) \text{ J m}^{-2}$.	90
4.2 Monthly mean noon time half-hourly UV-B flux for the period 1994-1999. Units are in W m^{-2} .	104
4.3 UV-Index computed from erythemal UV irradiances expressing its potential harmful effect.	110
4.4 Daily maximum erythemal UV irradiance at Penang and eleven other sites.	110

LIST OF FIGURES

Figures	Page
1.1 The annual mean global energy budget for the Earth-atmosphere system. The figures are percentages of the energy of the incoming solar radiation.	2
1.2 Absorption spectra for H ₂ O, CO ₂ , O ₂ , N ₂ O, CH ₄ and the absorption spectrum of the atmosphere.	3
1.3 Spectrum of ultraviolet radiation at top of atmosphere and at the surface of Earth for 300 Dobson Units of ozone.	5
2.1 (a) Model UVB-1 Ultraviolet Pyranometer. (b) Eppley Ultraviolet Photometer. (c) CM 11 Pyranometer. (d) The CM 11 Pyranometer mounted in a shadow ring stand (CM 121). The combination of a pyranometer and the shadow ring offers a simple solution to the problem of measuring diffuse radiation from the sky.	16
2.2 Operation principle of the UVB-1 pyranometer.	18
2.3 Relative spectral response of the UVB-1 instrument plotted together with the Parrish and CIE (Diffey) erythral action spectra.	19
2.4 Plot of UVB-1 instrument readings against measured integrated spectral data to formulate calibration constant.	20
2.5 UVB-1 instrument conversion factors (relative to the value at solar zenith angle of 30°). Solid horizontal lines show 5% deviations, dashed horizontal lines 10% deviations.	23
2.6 Relative spectral response of photocell sensor in the UV radiometer (photometer).	25
2.7 The photometer tower block. The metal structure is situated at the back of the Astronomy and Atmospheric Science Research Unit building, University of Science Malaysia.	28
2.8 Data logger setup.	33

2.9	UVB-1 instrument calibration.	36
2.10	Time series of half-hourly UV-A irradiance as measured by the reference unit in September 1994 and March 1999.	40
3.1	Time series of daily total global radiation (1994-1999).	49
3.2	Variation of monthly mean daily total global radiation for the period 1994-1999.	52
3.3	Annual variation of the monthly mean global radiation and the related observational meteorological parameters at Penang.	54
3.4	Monthly mean daily total global radiation for the period 1994-1999.	55
3.5	Comparison of diurnal monthly mean values of daily total global radiation under all sky conditions at some major cities in Malaysia.	56
3.6	Monthly mean half-hourly global flux (for all sky conditions).	59
3.7	Monthly mean half-hourly global flux for 1994-1999.	61
3.8	Six year mean of monthly mean half-hourly global flux (1994-1999).	63
3.9	Interannual variation of noon time global solar irradiance.	65
3.10	Monthly mean daily total measured global radiation from 1994 to 1999 for cloudless sky days, extraterrestrial solar radiation and clearness index for Penang.	71
3.11	Comparison of daily total global radiation values under cloudless conditions with predicted values.	76
3.12	Variation of monthly mean daily total diffuse radiation for the period 1994-1999.	78
3.13	Six year mean of the half-hourly diffuse flux for all sky conditions (1994-1999).	79
3.14	The average daily total UV-A radiation over the period 2000-2001.	82
3.15	Variation of monthly mean daily total UV-A radiation.	83
3.16	Monthly mean half-hourly UV-A flux for 2000-2001 for all sky conditions.	86
4.1	Time series of daily total UV-B radiation in the period from 1994 to 1999.	89

4.2	Relationship between the measured daily total UV-B and global radiation.	92
4.3	Variation of monthly mean daily total UV-B radiation.	93
4.4	Monthly mean half-hourly UV-B flux for all sky conditions.	95
4.5	Monthly mean half-hourly UV-B flux for 1994-1995 and 1998-1999.	98
4.6	Monthly mean half-hourly UV-B irradiance ($W\ m^{-2}$) for the period 1994-1995 and 1998-1999.	99
4.7	Four year mean of monthly mean half-hourly UV-B flux (1994-1995 and 1998-1999).	101
4.8	Seasonal variation of noon time solar ultraviolet-B radiation.	102
4.9	Time series of monthly mean half-hourly noon time UV-B irradiance at Penang from 1994 to 1999.	105
4.10	Daily total solar UV-B radiation on a horizontal surface for cloudless sky days during the 1994-1995 and 1998-1999 period.	107
4.11	Variation of the erythemal UV-B flux with time of day on a typical clear day in March, June, September and December.	111
4.12	Annual variation of the mean daily total effective UV-B and global radiation dosage as measured at Penang, together with related meteorological parameters and solar declination.	115
4.13	Relationship between fractional UV dose with percent cloud cover of the sky. The UV-B transmission is a strong function of cloud cover.	120
5.1	Schematic of steps in calculating the surface level solar UV-B irradiance (spectral model).	127
5.2	Daily total solar UV-B radiation on a horizontal surface for cloudless sky days during the period 1994-1995 and 1998-1999 compared to calculated values.	148
5.3	Comparison of the empirical model with measured monthly mean erythemal UV radiation at Penang.	153

NOMENCLATURE

β	Ångström turbidity coefficient
τ	Atmospheric optical depth
ϕ	Geographic latitude, north positive (degrees)
ω	Local hour angle
φ	Phase constant (day number 80)
δ	Solar declination
α	Wavelength exponent in Ångström turbidity equation
λ	Wavelength of radiation
ρ_λ	Sky albedo
ρ_λ'	Ground albedo
τ_λ	Total optical depth at wavelength λ
α_1	Coefficient of skewness
$\tau_{a,\lambda}$	Atmospheric aerosol optical depth
θ_n	Day angle
$\tau_{\text{NO}_2,\lambda}$	NO ₂ optical depth
ω_o	Single scattering albedo
$\tau_{\text{oz},\lambda}$	Ozone optical depth
ω_s	Sunrise hour angle
$\tau_{\text{SO}_2,\lambda}$	SO ₂ optical depth
θ_z or θ	Solar zenith angle
a	Radius of a spherical particle
$a_{\text{oz},\lambda}$	Spectral absorption coefficient for ozone
c	Percent cloud cover
D_c	Effective UV-B dose when percent cloud cover is c
D_n	Day number of year, 1 on 1 January, February is counted as having 28 days
D_o	Clear sky effective UV-B dose
e	Eccentricity correction factor of the Earth's orbit
E	Mean erythemal dosage
EQT	Equation of time
F_r	Forward scatterence factor associated with Rayleigh scattering
GMT	Greenwich mean time
H_A	Daily total UV-A radiation
H_B	Daily total UV-B radiation
H_G	Daily total Global radiation
H_o	Extraterrestrial daily total radiation on a horizontal surface
I	Extraterrestrial solar irradiance
I_λ	Spectral extraterrestrial irradiance at wavelength λ
$I_{d,\lambda}$	Directly transmitted spectral irradiance

$I_{d,\theta,\lambda}$	Direct spectral UV irradiance of solar radiation on a horizontal surface
$I_{g,\theta,\lambda}$	Spectral global UV irradiance of solar radiation on a horizontal surface
I_o	Solar irradiance on a horizontal surface
$I_{o,\lambda}$	Spectral irradiance of solar radiation on a horizontal surface above the atmosphere
$I_{s,\theta,\lambda}$	Diffuse spectral UV irradiance
$I_{s,a,\lambda}$	Diffuse spectral UV irradiance produced by aerosol scattering
$I_{s,m,\lambda}$	Diffuse spectral UV irradiance produced by multiple reflections between the ground and the atmosphere
$I_{s,R,\lambda}$	Diffuse spectral UV irradiance produced by Rayleigh scattering
K	Global clearness index
$k_{i,\lambda}$	Spectral attenuation coefficient for a single atmospheric process i
L	Longitude
MMS	Malaysian Meteorological Service
m	Air mass between the surface and top of the atmosphere
m_c	Pressure-corrected relative air mass
m_r	Relative optical air mass
n	Refractive index of particle
P	Measured surface pressure
P_o	Atmospheric pressure at sea level (1013 mb)
R_n	Earth-Sun distance on day D_n
R_o	Average Earth-Sun distance
S	Solar constant
ρ	Surface albedo
T_λ	Spectral atmospheric transmittance
$T_{a,\lambda}$	Transmittance of the direct spectral irradiance for absorption due to scattering and absorption by aerosol particles
$T_{aa,\lambda}$	Spectral transmittance of aerosols due to absorption
$T_{as,\lambda}$	Spectral transmittance of aerosols due to scattering
$T_{i,\lambda}$	Transmittance due to a single atmospheric process i
$T_{ma,\lambda}$	Total spectral transmittance due to molecular absorbers
$T_{NO_2,\lambda}$	Transmittance of the direct spectral irradiance for absorption by nitrogen dioxide
$T_{oz,\lambda}$	Transmittance of the direct spectral irradiance for absorption by ozone
$T_{R,\lambda}$	Transmittance of the direct spectral irradiance for absorption due to scattering air by molecules (Rayleigh scattering)
$T_{SO_2,\lambda}$	Transmittance of the direct spectral irradiance for absorption by sulphur dioxide
u_{oz}	Ozone column in atm-cm

TERMINOLOGY

Absorption cross-section is a measurement of an atom or molecule's ability to absorb light at a specified wavelength, measured in square cm/particle.

Albedo is a measure of reflectivity of a surface or body. It is the ratio of electromagnetic radiation reflected to the amount incident upon it. The fraction, usually expressed as a percentage from 0% to 100%

Dobson units (DU) are the standard way to express ozone amounts in the atmosphere. One DU is 2.7×10^{16} ozone molecules per square centimetre, or $2.7 \times 10^{20} \text{ m}^{-2}$. One Dobson unit refers to a layer of ozone that would be 10 micrometre thick under standard temperature and pressure.

Equinox - Twice during the year, September 21 and March 21, the length of day and night are equal because the tilt of the Earth's axis (in relationship to the sun) is nullified and both the Northern and Southern Hemispheres receive equal quantities of sunlight.

Extinction coefficient is a measure of the rate of the reduction of transmitted light through a substance.

Intensity is a measure of the time-averaged energy flux. (Unit: watt/m²).

Irradiance is the total radiant flux received on a unit area of a given surface. Also called the radiant flux density.

Optical depth is a measure of transparency, and is defined as the fraction of radiation that is scattered between a point and the observer.

Radiance is a physical quantity used to measure the intensity of a light beam, defined as power per unit solid angle per unit projected area. The SI unit of radiance is the watt per steradian per square metre ($\text{W m}^{-2} \text{ sr}^{-1}$).

Radiant energy is energy in the form of electromagnetic waves. Radiant energy may be calculated by integrating radiant power with respect to time. Radiant energy is usually expressed in joules.

Radiation generally means the transmission of waves from a source into a surrounding medium.

Refractive index of a material is the factor by which electromagnetic radiation is slowed down (relative to vacuum) when it travels inside the material.

Transmittance is the fraction of incident light at a specified wavelength that passes through a sample.

Turbidity is a cloudiness or haziness of the atmosphere caused by individual particles that are too small to be seen without magnification.

Zenith is the point in the sky which appears directly above the observer. More precisely, it is the point on the sky with a altitude of +90 Degrees.

ABSTRAK

SINARAN ULTRALEMBAYUNG-B (UV-B) SURIA PADA PERMUKAAN BUMI DI PULAU PINANG

Pengukuran fotometrik jalur lebar bagi sinaran ultralembayung-B (UV-B), ultralembayung-A (UV-A), global dan berbaur suria telah dibuat di Universiti Sains Malaysia (USM) dari tahun 1994 sehingga 2001. Kajian ini menunjukkan bahawa variasi besar temporal untuk ukuran sinaran suria adalah disebabkan kesan dominan sudut zenit suria dan awan. Bagi semua jenis keadaan langit, min jumlah sinaran harian untuk sinaran UV-B, UV-A dan global ialah $1.514 \times 10^4 \text{ J m}^{-2}$, $4.69 \times 10^5 \text{ J m}^{-2}$ dan $1.80 \times 10^7 \text{ J m}^{-2}$ masing-masing. Pada hari tanpa awan, keamatan sinaran maksimum harian bagi UV-B dan global ialah 1.372 W m^{-2} dan 1.423 kW m^{-2} . Ukuran sinaran UV-B berkesan telah ditukarkan kepada fluks UV eriterma untuk dikaitkan dengan kesan keupayaan berbahaya akibat pendedahan UV. Aras tertinggi fluks UV-B adalah antara masa 1030 dan 1530 jam waktu tempatan.

Kajian variasi harian untuk sinaran UV-B, UV-A dan global menunjukkan bahawa bagi sudut zenit yang sama, sinaran suria selepas tengah hari adalah lebih besar berbanding dengan sinaran sebelum tengah hari. Kesan tak simetri ini adalah disebabkan penyerakan sinaran suria oleh awan. Kajian mengenai variasi musim untuk sinaran UV-B, UV-A dan global menunjukkan perubahan berkala dengan sinaran suria maksimum

pada bulan Mac dan September. Kesan-kesan terhadap aras sinaran UV-B di permukaan Bumi juga telah dikaji dengan menggunakan parameter meteorologikal yang sedia ada. Satu model matematik untuk menganggarkan aras sinaran UV-B di permukaan Bumi juga telah dihasilkan dan dibandingkan dengan dua model terkenal. Pencapaian model spektral didapati adalah baik dengan ralat min sebesar 9.9%. Sebagai kajian tambahan, suatu model empirik yang ringkas telah dihasilkan dengan menggunakan kaedah analisis multivariat. Ralat min bagi model empirik adalah 2.5%

ABSTRACT

SURFACE LEVEL SOLAR ULTRAVIOLET-B RADIATION AT PENANG

Broadband photometric measurements of solar UV-B, UV-A, global and diffuse radiation were made at Universiti Sains Malaysia (USM), Penang from 1994 to 2001. Results from this study show that the large temporal variations for the measured solar radiation is due to the dominant effect of solar zenith angle and clouds. Under all sky conditions, the mean daily total radiation values for the UV-B, UV-A and global radiation were $1.514 \times 10^4 \text{ J m}^{-2}$, $4.69 \times 10^5 \text{ J m}^{-2}$ and $1.80 \times 10^7 \text{ J m}^{-2}$ respectively. For cloudless sky days, the daily maximum UV-B and global irradiance were 1.372 W m^{-2} and 1.423 kW m^{-2} . The measured effective UV-B irradiance was converted to the erythemal UV flux to relate it to the potential harmful effects due to UV exposure; UV-B flux level is in the High or Extreme ranges between 1030 and 1530 hours local time.

A study of the diurnal variation of the solar UV-B, UV-A and global radiation show that for similar zenith angles, the solar irradiance after solar noon is larger than that before solar noon. This asymmetrical effect is attributed to the scattering of solar radiation by clouds. Seasonal variation studies show a constant periodicity for the solar UV-B, UV-A and global flux with maximums in March and September. Using available meteorological parameters and total column ozone data, their effects on the surface level solar UV-B radiation was investigated. A mathematical model to estimate

the surface level solar UV-B radiation was also developed and compared with two established model. The spectral model performance is good with a mean error of 9.9%. To compliment the spectral model, a simple empirical model was also formulated using multivariate analysis. The mean error of the empirical model was 2.5%.

Chapter 1 : Introduction

Almost all the radiative energy entering the earth's atmosphere comes from the sun. The incoming solar radiation covers the entire electromagnetic spectrum from gamma and X-rays, through ultraviolet, visible, and infrared radiation to microwaves and radiowaves. Of the solar energy reaching the earth, 99 percent has a wavelength between 150 and 4000 nm, with 9 percent in the ultraviolet ($\lambda < 400$ nm), 49 percent in the visible ($400 < \lambda < 700$ nm) and 42 percent in the infrared ($\lambda > 700$ nm) (Houghton, 1985). As shown in Figure 1.1, of the total incoming solar radiation, 16 percent is absorbed by ozone in the stratosphere (stratospheric ozone), tropospheric water vapour and aerosols, 3 percent by clouds, and 51 percent by the earth's surface. The remaining 30 percent of solar radiation are backscattered by the air (6 percent), reflected by clouds (20 percent) and reflected by the earth's surface (4 percent) (Peixoto and Oort, 1992). The shaded areas in Figure 1.2 represent absorption of radiation due to various gases when it travels vertically through the atmosphere under clear conditions.

The UV spectra is usually divided into three groups: UV-C ($\lambda < 280$ nm), UV-B (280 nm $< \lambda < 320$ nm) and UV-A (320 nm $< \lambda < 400$ nm) (Meier et al., 1997). There is virtually no solar radiation reaching the earth's surface at wavelengths of less than 295 nm, as a result of strong absorption by atmospheric ozone and oxygen, whereas at UV wavelengths greater than 320 nm (UV-A range), the ozone absorption is small, and Rayleigh scattering and line absorption by other constituents are the main extinction processes (Kudish and Evseev, 2000). The UV radiation spectrum at the top of the atmosphere and at the surface of earth for 300 Dobson Units of ozone is shown in

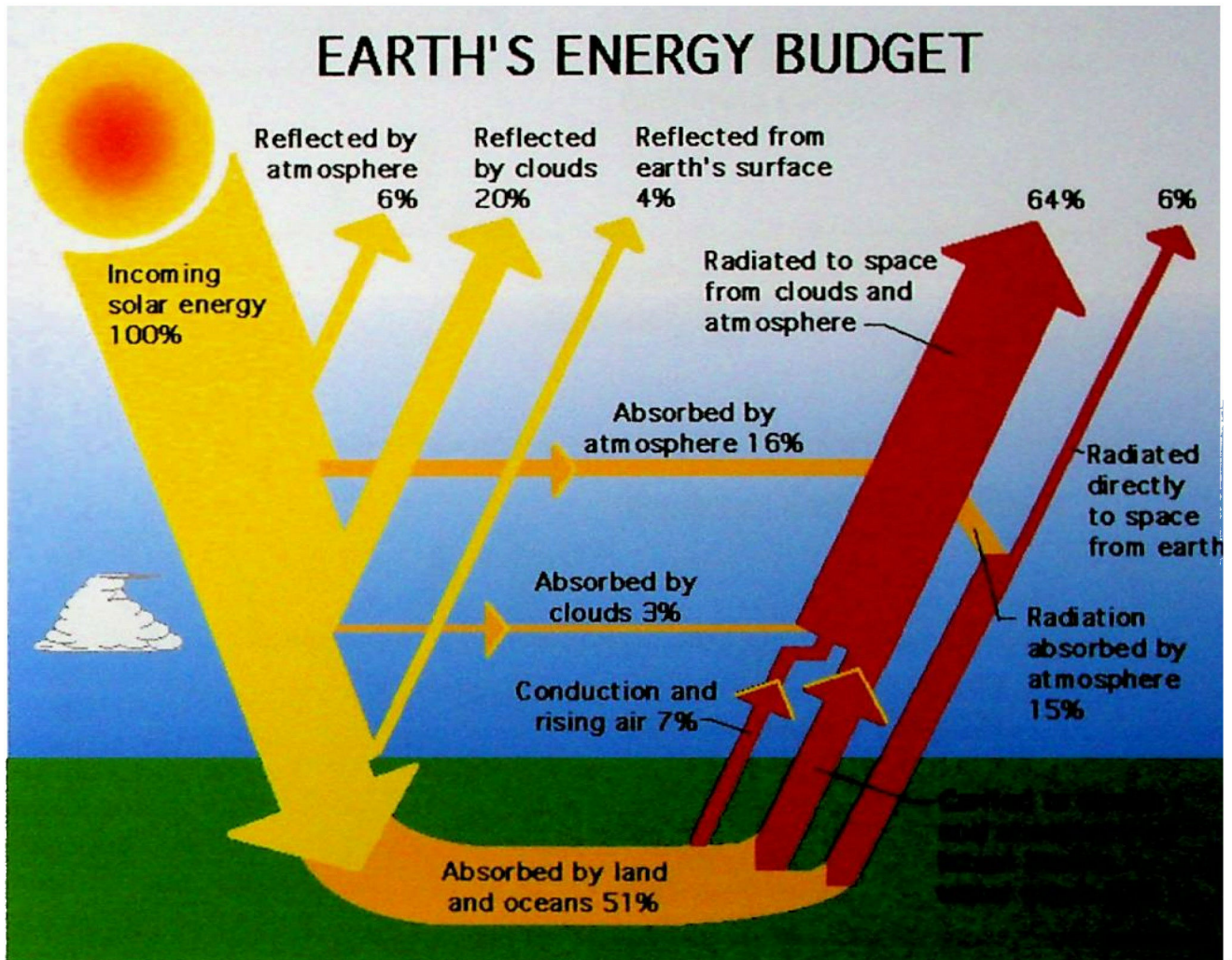


Figure 1.1. The annual mean global energy budget for the Earth-atmosphere system. The figures are percentages of the energy of the incoming solar radiation. (Peixoto and Oort, 1992)

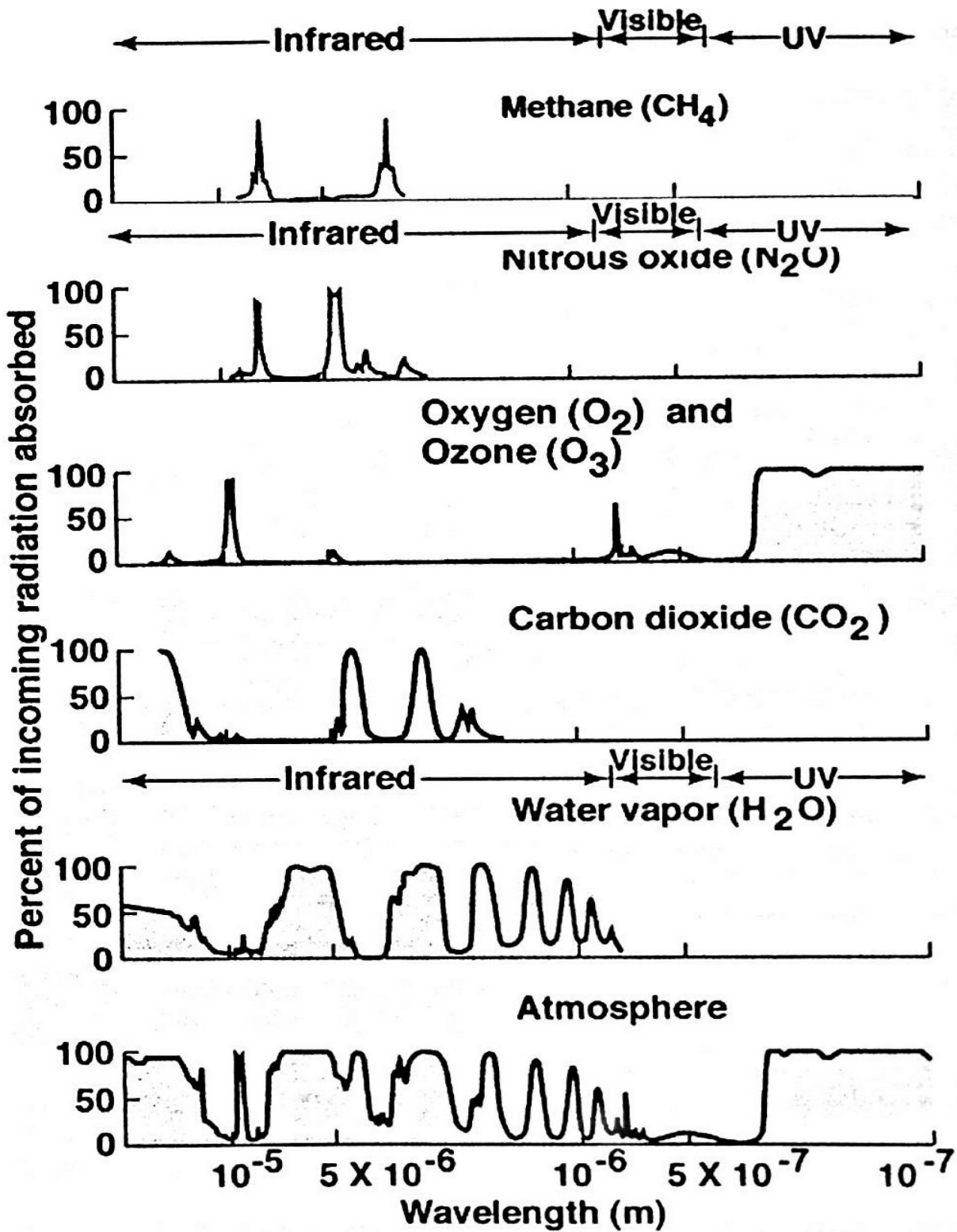


Figure 1.2. Absorption spectra for H_2O , CO_2 , O_2 , N_2O , CH_4 and the absorption spectrum of the atmosphere (Coulson, 1975).

Figure 1.3. Any depletion of ozone in the stratosphere will increase the ultraviolet flux reaching the biosphere (Pérez et al., 2002). This increase will be completely contained within the UV-B (Frederick et al., 2001) range. The inverse relationship between decreasing ozone amount and increasing level of UV-B radiation has been well established in both theory and measurements (Kerr and McElroy, 1993; Feister and Grewe, 1995; Varotsos et al., 1995; Kirchhoff et al., 1997a).

1.1 Attenuation of Surface Level Solar Ultraviolet Radiation

The intensity of solar ultraviolet radiation at ground level is dependent on earth-sun geometric factors and on a variety of atmospheric factors. Among the factors that contribute to UV-B attenuation are: Earth-Sun distance, solar zenith angle, total column ozone concentration, total column aerosol concentration, cloud properties, tropospheric constituents (such as nitrogen dioxide and sulphur dioxide), altitude above mean sea level and UV surface albedo (WMO, 1994; McKenzie et al., 2001; Lam et al., 2002; Palancar and Toselli, 2004). Because of the combined involvement of all these parameters in controlling the surface level solar UV radiation, it is difficult to determine absolutely the role of each parameter. Stratospheric components which effect the ground level UV-B irradiance are molecular scattering, absorption by ozone and scattering by aerosols (Pérez et al., 2002). Tropospheric factors include molecular scattering, absorption by gaseous pollutants, and scattering by aerosols and clouds (Acosta and Evans, 2000; Kaufman et al., 1998). Irradiance reaching the earth's surface at wavelengths greater than 330 nm is dominated by molecular and aerosol scattering, with ozone absorption being the major influence at wavelengths below 310 nm (Wang and Lenoble, 1994).

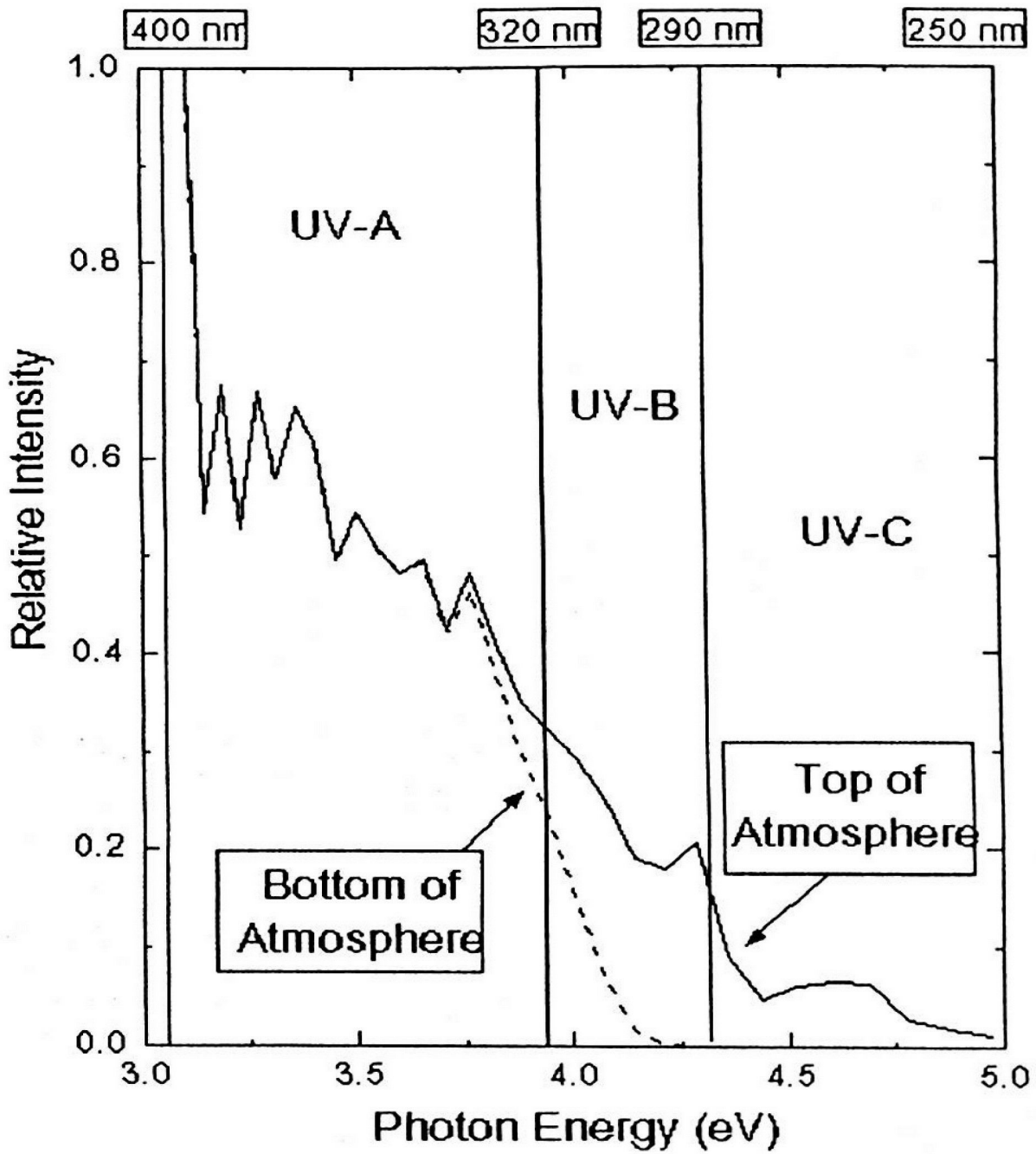


Figure 1.3. Spectrum of ultraviolet radiation at top of atmosphere and at the surface of Earth for 300 Dobson Units of ozone (Coulson, 1975).

1.2 Relevance of Solar Ultraviolet Radiation Measurements

Ozone depletion and the associated increase in solar ultraviolet radiation reaching the earth's surface is a major environmental, medical and scientific issue. A change in UV climate can cause adverse effect on the biosphere. On humans, all exposed tissue, especially the skin and eyes, can be harmed by ultraviolet radiation (Diffey and Oakley, 1987; Rosen et al., 1990; Leyden, 1990; Armstrong and Krickler, 1993; Wee et al., 1997). On terrestrial ecosystems, elevated levels of UV-B are known to inhibit plant growth, development and physiological processes (Caldwell et al., 1998; Pinto et al., 1999). Photodegradation of materials, such as synthetic polymers (plastics and elastomers), are mainly due to ultraviolet-B radiation (Halvorson and Kerr, 1994; Andradý et al., 1995). These potential effects of enhanced ultraviolet radiation on photobiological and photochemical processes could lead to socioeconomic consequences. In assessing this impact, studies on the modification of solar ultraviolet-B by stratospheric ozone, and geometric and environmental factors are important. This will require accurate and sustained monitoring of UV fluxes.

Although solar UV-B irradiance data collection for the higher latitudes have been carried out intensively at many locations for many years now (Wardle et al., 1994; Diaz et al., 1997; WMO, 1999), however it is not the same for the equatorial/tropical regions. At the tropical latitudes, the erythemally-weighted irradiance far exceeds that incident at higher latitudes (Frederick and Erlick, 1994). At the Antarctic latitudes, even during the occurrence of the ozone hole, direct transmission of UV radiation of wavelength higher than 290 nm remains lower than at the tropics (Davies, 1993; Ilyas et al., 1999).

1.2 Relevance of Solar Ultraviolet Radiation Measurements

Ozone depletion and the associated increase in solar ultraviolet radiation reaching the earth's surface is a major environmental, medical and scientific issue. A change in UV climate can cause adverse effect on the biosphere. On humans, all exposed tissue, especially the skin and eyes, can be harmed by ultraviolet radiation (Diffey and Oakley, 1987; Rosen et al., 1990; Leyden, 1990; Armstrong and Kricger, 1993; Wee et al., 1997). On terrestrial ecosystems, elevated levels of UV-B are known to inhibit plant growth, development and physiological processes (Caldwell et al., 1998; Pinto et al., 1999). Photodegradation of materials, such as synthetic polymers (plastics and elastomers), are mainly due to ultraviolet-B radiation (Halvorson and Kerr, 1994; Andradý et al., 1995). These potential effects of enhanced ultraviolet radiation on photobiological and photochemical processes could lead to socioeconomic consequences. In assessing this impact, studies on the modification of solar ultraviolet-B by stratospheric ozone, and geometric and environmental factors are important. This will require accurate and sustained monitoring of UV fluxes.

Although solar UV-B irradiance data collection for the higher latitudes have been carried out intensively at many locations for many years now (Wardle et al., 1994; Diaz et al., 1997; WMO, 1999), however it is not the same for the equatorial/tropical regions. At the tropical latitudes, the erythemally-weighted irradiance far exceeds that incident at higher latitudes (Frederick and Erlick, 1994). At the Antarctic latitudes, even during the occurrence of the ozone hole, direct transmission of UV radiation of wavelength higher than 290 nm remains lower than at the tropics (Davies, 1993; Ilyas et al., 1999).

To understand the relationship between factors that influence ground level ultraviolet radiation, reliable data of good quality is required. Development of a sound ultraviolet climatology will provide the user community (environmentalists, medical scientists, ecologists, meteorologists, policy makers) much needed information to enable them to study the effects, understand responses of living systems and to develop strategies, evaluate possible ultraviolet trends and for forecasting purposes. Therefore, it is essential to obtain spatial and temporal changes of UV radiation. Data that is of known quality will be an important tool in predictive capabilities, verification of modeled estimations and improve our understanding of atmospheric processes, especially in the equatorial region. To this effect, a reliable calibration of the instrument is required to compare results from different observation sites. This will then help the international scientific community to form a global ultraviolet climatology picture.

One of the important byproduct of solar ultraviolet measurement and research will be to create public awareness to the risks of overexposure to solar ultraviolet radiation. According to WMO (1994), the erythemal UV irradiance in the low latitudes are more than twice the values measured in the high latitudes. The possible detrimental health effects of exposure or overexposure to solar ultraviolet radiation is well documented (UNEP, 1989, 1994 and 1998; WHO, 1994). Measures have to be taken to educate the public to change their behavior in the amount of time exposed to sunlight. This can be done in the form of a UV Index (detailed discussions are in Chapter 5). Solar UV data has also been increasingly used to study air pollution (Galindo et al., 1995).

1.3 UV Measurements

The discovery of the ozone hole over Antarctica in 1985 (Farman et al., 1985) and subsequent reports that confirm the depletion of the stratospheric ozone (WMO, 1989; WMO, 1992) brought world-wide concern of the possible impacts of increased surface level ultraviolet radiation. Since then many establishments and countries have initiated programmes to monitor surface level ultraviolet radiation (Weatherhead and Webb, 1997). Various types of instruments are been used for this purpose - broadband, narrowband or spectral. These instruments are stationed on ground or mounted on aircraft or satellite (Meerkoetter et al., 1997; Lubin et al., 1998). Extensive research on the physics of solar ultraviolet radiation and their variations due to natural and anthropogenic causes have also been carried out (Forster, 1995; Bodeker and McKenzie, 1996; Kirchhoff et al., 2001). Two world bodies, World Health Organization (WHO) and United Nations Environment Programme (UNEP) have been actively involved in solar ultraviolet study activities.

In the United States, there are four main agencies monitoring UV-B radiation, namely the United States Department of Agriculture (USDA) (Gibson, 1994), the Environment Protection Agency (EPA) (Barnard and Cupitt, 1994), the National Science Foundation (NSF) (Booth et al., 1994) and the National Oceanic and Atmospheric Administration (NOAA). Environment Canada (EC) measures spectral ultraviolet irradiance at twelve locations in Canada (Wardle et al., 1994). In Europe, most countries have initiated programmes to monitor solar ultraviolet radiation since the seventies and eighties. The Nordic countries have established a working group for ozone and UV research in 1988 (NOG). Other European countries do have their own monitoring systems (Webb, 1992;

Wester, 1992; Borkowski, 1994; Matthes, 1994; Leszczynski et al., 1994). The Australian Radiation Laboratory (ARL) has been involved in the measurement of solar ultraviolet radiation since the early 1980's (Gies et al., 1994). In the late 1980's, a New Zealand-wide network of filter instruments (International Light Inc.) was established (McKenzie et al., 1993). This ultraviolet radiation programme was initiated by the National Institute of Water and Atmospheric Research (NIWA). In South America, there exists a network for monitoring the solar ultraviolet-B radiation. The network stations are located at Punta Arenas (Chile) (Kirchhoff et al., 1997a), La Paz (Bolivia) (Andrade et al., 1997) and Natal (Brazil) (Kirchhoff et al., 1997b). In the polar regions, the National Science Foundation of America has installed a network for UV-B measurements in 1988. Presently it includes three stations in Antarctica (South Pole, McMurdo and Palmer), one at Ushuaia (Argentina) and one in Alaska (Barrow) (Diaz et al., 1997).

Many countries in Asia have also started monitoring of solar ultraviolet radiation. Japan Meteorological Agency (JMA) started routine observations of solar spectral ultraviolet irradiance at Tsukuba since 1 January 1990 and at Sapporo, Kagoshima and Naha since 1 January 1991 (Ito et al., 1994). China have been conducting UV-B measurements at Mt. Waliguan (36.387° N, 100.898° E) since 1991 (Song et al., 1994). UV-B measurements in India were initiated around 1980 at the National Physical Laboratory (NPL), New Delhi and the Centre for Earth Sciences Studies (CESS) (Subbaraya, 1994). The magnitude of erythemal UV radiation levels measured at some of these sites are tabulated in Table 4.4. It is obvious that surface level UV radiation decrease with latitude. However, for similar latitudes, UV radiation levels increase with altitude.

In Malaysia, the Malaysian Meteorological Services (MMS) have been monitoring solar UV radiation since 1995 using a Brewer spectrometer. However, no papers have been published by MMS on this subject matter. At Universiti Sains Malaysia measurements of ground level solar ultraviolet radiation have been undertaken since 1978 (Ilyas and Appandi, 1979; Ilyas and Barton, 1983; Ilyas et al., 1988; Ilyas, 1992; Ilyas, 1993). In these previous studies, it was found that the global UV radiation is very high and that cloud cover is the dominant factor affecting the surface level radiation. But the lack of supporting *in situ* measurements of other meteorological parameters limited the discussions. The data could not be compared with other sites because calibration procedures were not discussed extensively in the reports produced. There were no measurements of surface level UV-B and diffuse solar radiation in the previous studies. However this study is the first comprehensive and integrated study over a time period of solar UV-B radiation in Malaysia.

1.4 Research Objectives

The objectives of this research are:

- (a) to produce good quality data of surface level solar ultraviolet-B radiation at Penang under well controlled parameters, and monitor solar ultraviolet-A, total global and total scattered radiation to provide reference information on solar radiation climatology,
- (b) to determine bench marks for solar UV-B and total global radiation at Penang so that it can be used for trend and/or impact studies in the future and in the design of solar energy applications,
- (c) to analyse the data obtained to interpret diurnal and seasonal variations,

- (d) to investigate the effects of ozone and other relevant meteorological parameters on the surface level UV-B radiation levels in an equatorial environment, and
- (e) to develop a mathematical model to estimate surface level solar UV-B irradiance for the equatorial /tropical regions using the Penang data as a case study.

1.5 Thesis Overview

This thesis consists of six chapters. A brief description of the literature survey on solar ultraviolet radiation is presented in Chapter 1. The research materials and methodology used is presented in Chapter 2. Besides detailed descriptions on installation, maintenance, and data retrieval and storage procedures, the various steps taken to calibrate the instruments have also been explained. Chapter 3 consists of results and discussions on global and scattered radiation, and UV-A radiation. An empirical model for the global solar radiation have also been developed.

Chapter 4 details the data analysis procedures, UV-B radiation observational results and the effect of some major UV-B attenuating factors on the surface level UV-B radiation are discussed. For practical consideration, the basic UV-B irradiance has also been related to erythemal UV-B dosage for some discussions. In Chapter 5, a mathematical model is developed to estimate the surface level UV-B radiation at Penang. Chapter 6 concludes this thesis with a summary of the findings followed by recommendations for future research in this challenging field.

Chapter 2 : Experimental

A series of photometers have been used for studying the solar ultraviolet and total radiation. In this chapter, the details of various techniques available and the types of instruments used to measure the various solar radiation component fluxes reaching the surface level are discussed. Their principle of operation and optical characterization, installation, maintenance and data retrieval procedures used, together with method of calibration and sources of errors are briefly presented.

2.1 Introduction

The two main spectral bands of solar radiation received at the earth's surface are the short-wave ultraviolet (UV) and visible radiation. These radiation components are received both directly from the sun and from scattering in the clouds and atmosphere. Of particular interest is the UV portion of the solar radiation because of its negative effects on humans, terrestrial and aquatic ecosystems, and air quality (see section 1.2). The direct and diffuse irradiance from the upward hemisphere is measured using a pyranometer.

Generally, the accuracy of solar radiation measuring instruments depend on:

- (i) instrument's sensitivity, stability, linearity, spectral response and response time;
- (ii) change in response due to variation in ambient temperature, effect of auxiliary equipment, the directional response of the sensor on the elevation (cosine effect),

(iii) azimuth of the sun (azimuth effect) and the effect of inclination of the pyranometer (Iqbal, 1983).

The main problems in obtaining reliable solar radiation climatology measurements include (Iqbal, 1983):

- ◆ ambiguities in detector construction which fairly represents the sensitivity of different biological and chemical targets,
- ◆ difficulties of maintaining accurate field instrument calibrations over a period of many years, and
- ◆ the absence of a baseline, long-term historical solar radiation record.

Solar radiation measuring instrument detectors can be classified as calorimetric, thermomechanical, thermoelectric, or photoelectric (Iqbal, 1983).

- ◆ In the calorimetric instrument, the radiant energy is incident on a high-conducting metal with a nonselective black paint of high absorptance. The radiant energy is converted into heat that can be measured by a variety of means.
- ◆ In the instruments based on the thermomechanical principle, the radiant flux is measured through bending of a bimetallic strip.
- ◆ A thermoelectric device consists of two dissimilar metallic wires with their ends connected. An electromagnetic force (e.m.f.) is developed when the two junctions are at different temperatures.
- ◆ In the photoelectric sensors, a semiconductor p-n junction is used. When radiation at an energy level capable of ionizing the atoms is incident on the p-n junction, an electrical current arises from the continuous movement of excess electrons and

holes. This kind of detectors are lower in cost but have faster response times for instantaneous measurements.

Ground-based instruments measuring solar radiation components can be divided into three types (WMO, 1999):

(i) Broadband instruments

- the spectral response of these instruments matches that of a particular action spectrum. The main attractive feature of these instruments are its low cost and rapidity of measurements. Broadband meters provide an important source of information over wide geographic areas and over long time periods.

(ii) Multi-channel medium-spectral-resolution instruments

- the main advantage of these filter instruments are their ability to make nearly simultaneous measurements at many wavelengths. Therefore, they can be very useful for separating cloud and aerosol effects from ozone effects.

(iii) high-resolution spectrometers

- there are two types, namely filter and grating instruments. Their increased cost and maintenance is offset by the wealth of spectral detail available and their ability to independently determine ozone and aerosol amounts, and to estimate the extraterrestrial UV flux.

However in recent years, the role of satellites in measurements of surface level solar radiation, especially UV climatology is gaining wide acceptance. Frederick and Lubin (1988) have demonstrated that satellite measurements of atmospheric ozone and cloud reflectance may be used in conjunction with radiative transfer theory to compute the

budget of UV radiation in the Earth-atmosphere system. But such application will still need surface level data for validation.

2.2 Types of Radiation Instruments Used

In the present study, basically three different types of instruments were used for obtaining the solar radiation data. They are UVB-1 Pyranometer, Eppley UV Photometer and the CM 11 Pyranometer. The instrumentation utilized to measure the various solar radiation components in this study measures the radiation incident on a plane horizontal surface.

2.2.1 Solar UV-B Radiation

The solar UV-B radiation was measured using a Model UVB-1 Ultraviolet Pyranometer (Figure 2.1a) (the manufacturers are Yankee Environmental System, Inc.). The UVB-1 Pyranometer measures the power per unit area of UV-B radiation received by a horizontal surface from the entire hemisphere of the sky (global solar UV-B irradiance). It is a broadband UV-B detector with a spectral response range of 280 to 330 nm. The cosine response of the instrument is $\pm 5\%$ for 0 - 60 degree solar zenith angle, and a response time of 0.1 second. It's sensitivity is 1.97 Volt/(Watt/m²) of effective UV-B irradiance.

budget of UV radiation in the Earth-atmosphere system. But such application will still need surface level data for validation.

2.2 Types of Radiation Instruments Used

In the present study, basically three different types of instruments were used for obtaining the solar radiation data. They are UVB-1 Pyranometer, Eppley UV Photometer and the CM 11 Pyranometer. The instrumentation utilized to measure the various solar radiation components in this study measures the radiation incident on a plane horizontal surface.

2.2.1 Solar UV-B Radiation

The solar UV-B radiation was measured using a Model UVB-1 Ultraviolet Pyranometer (Figure 2.1a) (the manufacturers are Yankee Environmental System, Inc.). The UVB-1 Pyranometer measures the power per unit area of UV-B radiation received by a horizontal surface from the entire hemisphere of the sky (global solar UV-B irradiance). It is a broadband UV-B detector with a spectral response range of 280 to 330 nm. The cosine response of the instrument is $\pm 5\%$ for 0 - 60 degree solar zenith angle, and a response time of 0.1 second. Its sensitivity is $1.97 \text{ Volt}/(\text{Watt}/\text{m}^2)$ of effective UV-B irradiance.

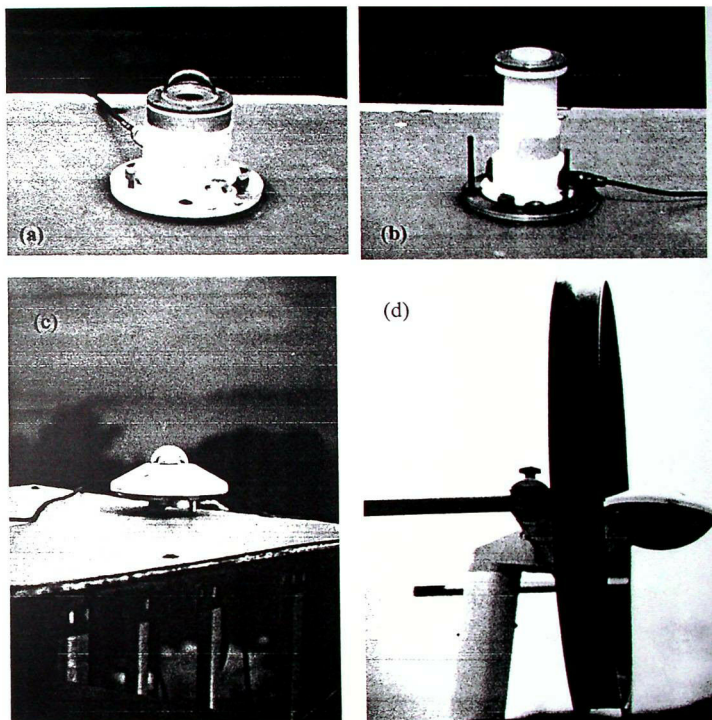


Figure 2.1. (a) Model UVB-1 Ultraviolet Pyranometer (b) Eppley Ultraviolet Photometer (c) CM 11 Pyranometer (d) The CM 11 Pyranometer mounted in a shadow ring stand (CM 121). The combination of a pyranometer and the shadow ring offers a simple solution to the problem of measuring diffuse radiation from the sky.

(a) Principle of Operation

The operation principle of the instrument is shown in Figure 2.2 (Dichter *et al.*, 1993). The measurement technique employed in the instrument utilizes colored glass filters and a UV-B sensitive phosphor to block all of the sun's visible light and convert the UV-B light into visible (green) light. The resulting green light is in turn measured by a solid state detector (photodiode). A two-stage amplifier circuit then converts the photodiode output current into a useable output voltage span (0-5 Vdc). The performance of the detector and phosphor are temperature dependent. They are therefore equipped with an internal temperature control system to maintain them at a fixed temperature. The instrument had been calibrated in the factory.

(b) Model UVB-1 Characterization

The instrument have been characterized using the calibration theory proposed by Grainger, Basher and McKenzie (1993). Comparisons of the spectral response of the instrument with the Parrish and CIE erythemal action spectra is shown in Figure 2.3. It can be seen that the spectral response is very similar to the International Commission of Illumination (CIE) human erythemal action spectra (Dichter *et al.*, 1993).

(c) Instrument Calibration Constant

A plot of UVB-1 instrument readings against the concurrently measured integrated spectral data is shown in Figure 2.4. The gradient of the linear regression line fitted to the points gives the calibration constant, K which has the value $1.968 \pm 0.011 \text{ V W}^{-1} \text{ m}^2$. After correction for the 5% uncertainty of the spectral irradiance measurement, the best value for K is $1.97 \pm 0.16 \text{ V W}^{-1} \text{ m}^2$.

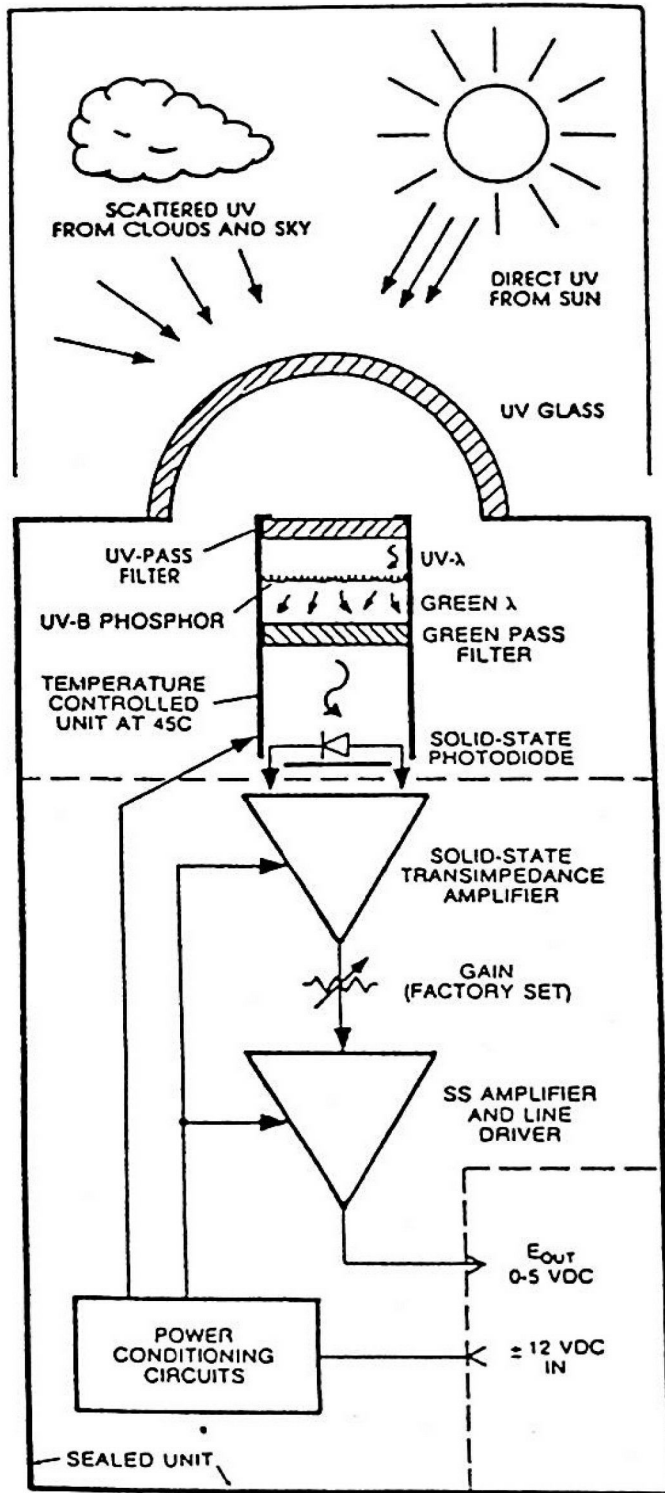


Figure 2.2. Operation principle of the UVB-1 pyranometer.

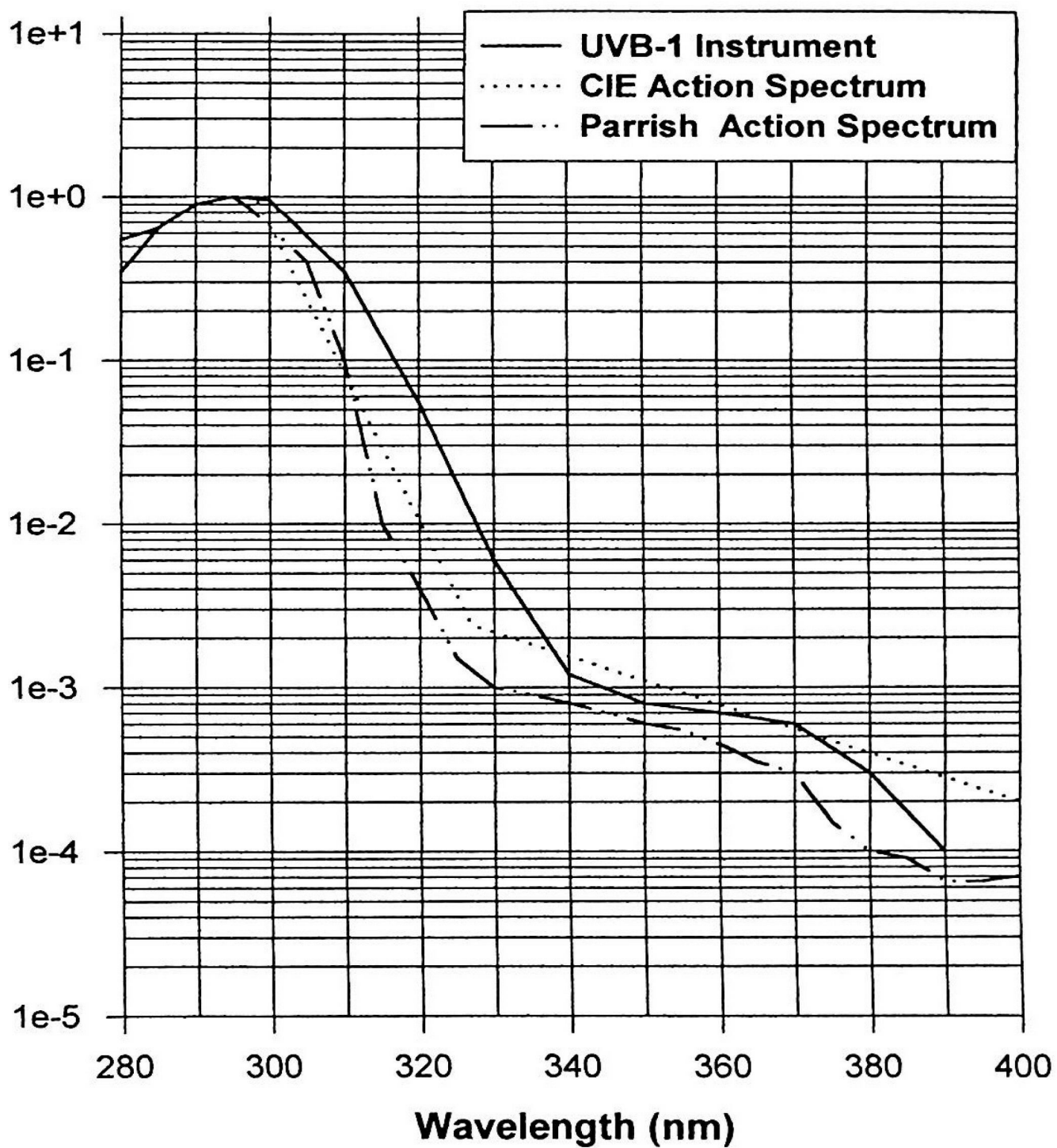


Figure 2.3. Relative spectral response of the UVB-1 instrument plotted together with the Parrish and CIE (Diffey) erythemal action spectra.

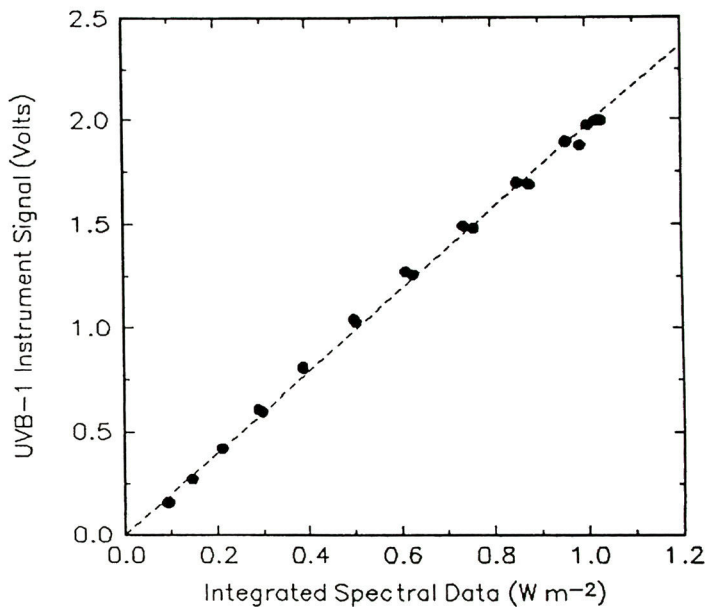


Figure 2.4. Plot of UVB-1 instrument readings against measured integrated spectral data to formulate calibration constant.

To convert the instrument output signal (in volts) to the irradiance of interest (total UV-B or erythemal, in $W m^{-2}$), the signal voltage is multiplied by a conversion factor provided by the manufacturer (Yankee Environmental Systems, 1991). The conversion factor is just the ratio of the energy measured by a detector with an ideal cosine and spectral response to the energy measured by the UVB-1 instrument. The conversion factors, which are relative to the value at solar zenith angle of 30° , are tabulated in Table 2.1 (The calibration angle to force the cosine error to be zero is 30°). The relative correction factor as a function of the solar zenith angle for the different types of irradiance is shown in Figure 2.5.

2.2.2 Solar UV-A Radiation

The solar UV-A radiation was measured using a TUVR Eppley ultraviolet photometer (serial number : 28289) (Figure 2.1b). The spectral range of this instrument is 295-385 nm. This photometer is widely used to monitor solar ultraviolet irradiance and has been extensively described (Drummond and Wade, 1969; Coulson, 1975). These authors have found that the instrument response is centered between 340 nm and 370 nm, and that ranges of 380-390 nm and 390-400 nm contribute only minor amounts to the total radiometer output, while significantly contributing to UV-A irradiance.

(a) Principle of Operation

The main component of the photometer are a Weston selenium barrier-layer photoelectric cell with a sealed-in quartz window, a bandpass filter and a Teflon diffuser disc. The bandpass filter serves to restrict the wavelength response of the

TABLE 2.1. Detailed tabulation of conversion factors for total UV-B and erythema irradiance. Units are in $W\ m^{-2}\ V^{-1}$. Erythema is the reddening of the untanned skin caused by the UV-B radiation. The Commission Internationale de L'Eclairage (CIE) human erythema action spectrum, shown in Figure 2.3, is given by McKinlay and Diffey (1987). Another widely used erythema action spectrum is given in the work of Parrish (1982) (see Figure 2.3).

Solar Zenith Angle	Total UV-B		Erythema	
	280 - 315 nm	280 - 320 nm	Diffey	Parrish
21.8	1.060	1.907	0.144	0.158
25.0	1.078	1.953	0.143	0.158
30.0	1.093	2.006	0.141	0.157
35.0	1.102	2.060	0.139	0.154
40.0	1.103	2.105	0.138	0.150
45.0	1.108	2.164	0.136	0.145
50.0	1.112	2.240	0.136	0.139
55.0	1.115	2.338	0.137	0.134
60.0	1.130	2.494	0.140	0.131
65.0	1.126	2.658	0.145	0.126
70.0	1.104	2.859	0.145	0.125

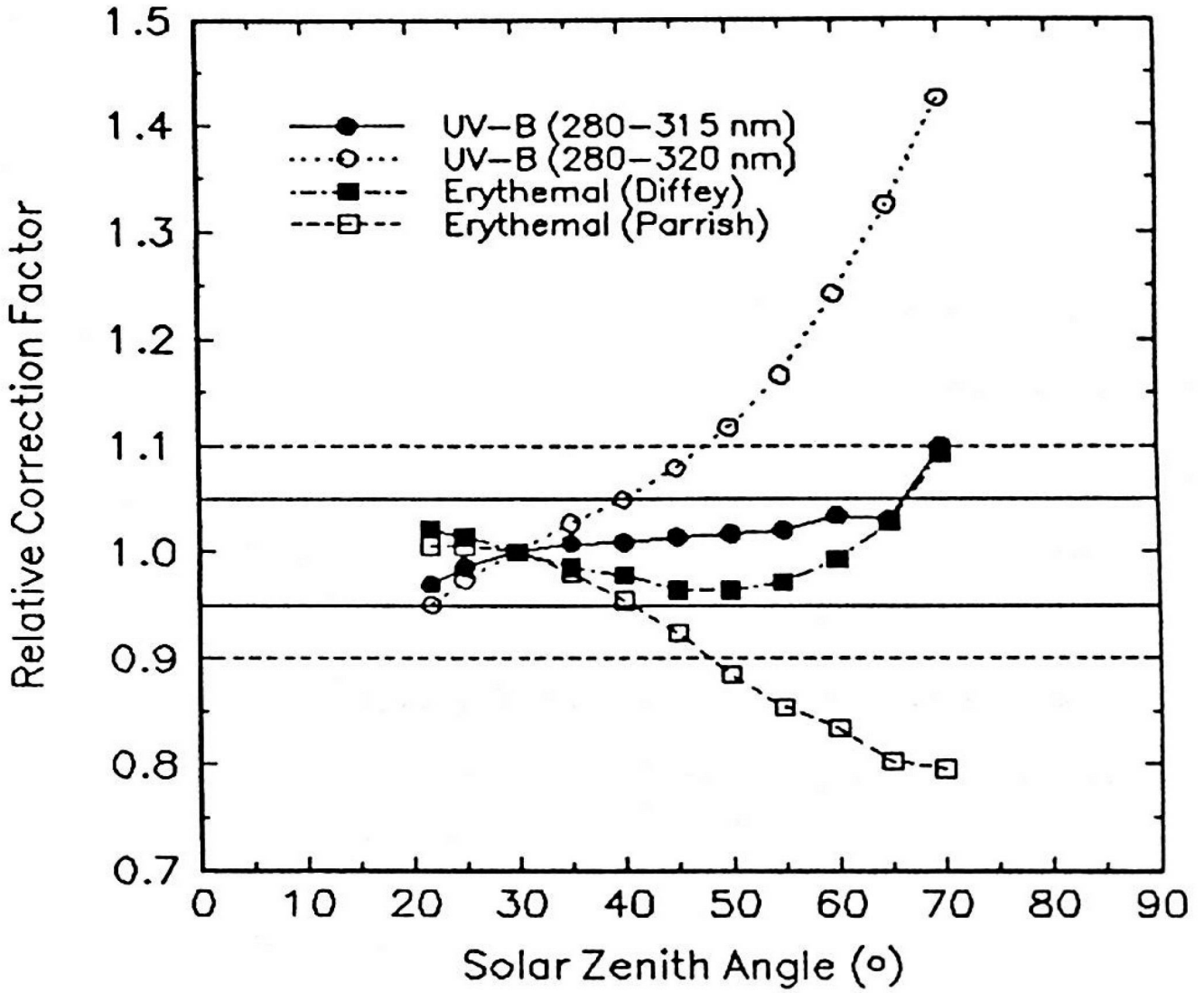


Figure 2.5. UVB-1 instrument conversion factors (relative to the value at solar zenith angle of 30°). Solid horizontal lines show 5% deviations, dashed horizontal lines 10% deviations.